Spectroscopy 17 (2003) 213–230
IOS Press

β-hairpin polypeptides by design and selection

Nicholas J. Skelton *, Tamas Blandl, Stephen J. Russell, Melissa A. Starovasnik and Andrea G. Cochran

Department of Protein Engineering, Genentech Inc., 1 DNA Way, South San Francisco, CA 94080, USA

Abstract. We have developed polypeptide scaffolds that readily adopt a β-hairpin conformation (a pair of antiparallel strands connected by a turn) in solution. The study of such peptides allows us to understand the factors that govern stability and folding of these motifs in proteins, and permits mimicry of functionally important regions of proteins. Spectroscopic and biophysical methods have been used to characterize the conformational preferences and stability of these peptides, with a strong emphasis on using restraints generated from ^{1}H NMR spectroscopy to determine their three-dimensional structure. By optimization of inter-strand interactions, we have developed highly stable disulfide-cyclized and linear β-hairpin peptides. In particular, tryptophan residues at non-hydrogen bonded strand sites (NHB) are highly stabilizing. A variety of turn types have been presented from these scaffolds, suggesting that they might generally be useful in turn presentation. Interestingly, β-hairpin peptides (containing a disulfide and a NHB tryptophan) have recently been discovered as antagonists of protein–protein interactions from naïve peptide libraries displayed on phage. Comparison of one such β-hairpin peptide with an α-helical peptide of very similar sequence provides further insight into the role that residue type and context play in determining polypeptide conformation.

1. Introduction

Polypeptide β-hairpins have been the subject of much study in recent years [11,16,27,44]. Although prevalent in folded proteins, designing short peptides that adopt a β-hairpin conformation using only naturally-occurring amino acids has not been straightforward. Thus, in contrast to the α-helical case where many of the underlying factors that stabilize helix formation have been understood from model peptide studies [7,38], less progress has been made in systematically understanding β-hairpins. The problem is a complex one due to the non-local nature of the stabilizing interactions and the variety of sites present, e.g. turn vs. strand and hydrogen bonding (HB) vs. non-hydrogen bonding (NHB) positions in the strands. Moreover, spectroscopic analysis is rarely able to quantitate β-hairpin content accurately, a problem compounded by the marginal stability and dynamic nature of many model β-hairpin peptides.

Key factors that influence the stability of a β-hairpin are (1) strand–strand interactions; (2) ability of residues connecting strands to adopt a turn conformation appropriate for hairpin formation and (3) mechanisms to tether the N- and C-termini of the polypeptide. In order to investigate the amino acid requirements at strand locations for optimum hairpin stability, we have developed a 10-residue model β-hairpin peptide whose central residues have moderate type II′ turn propensity and whose terminal cysteine residues are tethered by a disulfide bond [10]. In this system, the disulfide bond between the cysteine thiols will form more readily if there is a stable association of the antiparallel strands. Thus, measurement of the equilibrium constant for disulfide bond formation (or thiol effective concentration, C_{eff}) allows a free energy of folding to be determined (ΔG) and compared between different peptide analogs ($\Delta\Delta G$) [15,32,33]. In addition, we have also used conformation-dependent NMR parameters

*Corresponding author. Tel.: +1 650 225 6402; Fax: +1 650 225 3734; E-mail: skelly@gene.com.

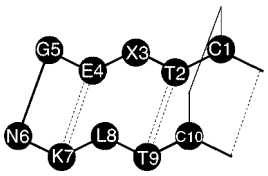

Fig. 1. Schematic view of the β-hairpin scaffold. The thick, thin and dotted lines indicate the peptide backbone, the disulfide bond, and cross strand hydrogen bonds, respectively.

to assess the degree of β-hairpin formation in the oxidized state, and to determine three-dimensional structures for the more stable peptides.

Using this scaffold, we have systematically substituted residues in non-hydrogen-bonded (NHB) strand sites (see Fig. 1) with most of the naturally occurring amino acids [10]. Large hydrophobic or aromatic side chains (especially tryptophan) were found to be very stabilizing, and the effects at the two NHB sites were independent and additive [42]. Substitutions at the adjacent HB sites also lead to improved stability, although in this case the two sites are not energetically equivalent. Using one of the more stable scaffolds, we have shown that a number of 2- and 3-residue turns can be used to connect the strands without loss of β-hairpin character [4,10]. We have also characterized the conformational properties of a CX_8C-containing peptide discovered from a naïve peptide phage display library. This peptide acts as an agonist of the erythropoietin receptor and adopts a β-hairpin conformation in the receptor-bound state [28]. Hybrids between this peptide and a peptide of very similar sequence that adopts an α-helical conformation in solution shed further light into the determinants of β-hairpin stability [50]. Finally, we have taken the feature that most stabilizes strand association in the CX_8C scaffold, a tryptophan at a non-hydrogen-bonded strand site, and used it to stabilize a β-hairpin in the absence of a disulfide bond [9]. These 12-residue, highly structured linear β-hairpin peptides, dubbed tryptophan zippers, are monomeric in solution and fold cooperatively, and as such, may be considered the smallest example yet described of a cooperatively folding tertiary structure (a "mini-protein").

Throughout this work, we have placed a strong emphasis on using NMR spectroscopy to characterize the peptides being studied. In this way, we can correlate the effects of stabilizing substitutions with particular structural features in the peptides. Moreover, the NMR data also give insights into the partial folding and internal dynamics of specific regions of a peptide. As a result, these investigations have furthered our understanding of the subtle interplay of side chain contacts that determine conformation in peptides and proteins. This knowledge may be used to design peptides that mimic the conformation of functionally important epitopes of intact proteins, and also in the design of peptide libraries (e.g. for use in phage display) that have a predefined conformational character.

2. Materials and methods

Peptide synthesis. Peptides were synthesized as C-terminal amides using standard Fmoc chemistry on a Pioneer synthesizer (PE Biosystems) as described previously [50].

Thiol effective concentration measurements. Equilibrium constants were measured relative to the reference thiol glutathione (GSH) at pH 8.1 and 20°C [10]. Briefly, concentrations of reduced and oxidized species were determined from HPLC peak areas, and effective concentrations (C_{eff}) were obtained from the following relationship: $C_{\text{eff}} = ([\text{GSH}]^2 \cdot [\text{peptide}_{\text{ox}}])/([\text{GSSG}] \cdot [\text{peptide}_{\text{red}}])$. The C_{eff} values re-

ported in Table 1 and Table 2 are averages from 3 or more HPLC analyses. Uncertainties in the $\Delta\Delta G$ values calculated from the C_{eff} values are less than 0.03 kcal mol^{-1}.

CD spectroscopy. Concentrations of peptide stock solutions were determined spectrophotometrically as described [10]. Samples contained 20 μM peptide in 20 mM potassium phosphate, pH 7.0. Spectra were acquired with an Aviv Instruments, Inc. Model 202 spectrophotometer at 5°C. Averaging time at each wavelength was 10 s.

NMR spectroscopy. NMR samples contained 3–9 mM peptide in 92% H_2O/8% D_2O pH 5.0–5.3 and ∼100 μM 1,4-dioxane as chemical shift reference. All spectra were acquired on Bruker Avance-500 or Avance-600 spectrometers at 10 or 30°C as described previously [6,48]. All analysis of NMR data was performed with the program FELIX (Accelrys, San Diego). Resonance assignments were made by standard methods using 2QF-COSY, TOCSY and ROESY data collected in H_2O solution [61]. ROESY and COSY-35 spectra were also acquired from D_2O solutions of the peptides. ^{13}C resonance assignments were obtained for some peptides using HMQC and ^{1}H-TOCSY HMQC spectra acquired from D_2O solution [6].

Structure calculations. Distance restraints were generated from H_2O and D_2O ROESY spectra (τ_m = 150 ms); dihedral angle restraints were derived from $^3J_{\text{HN-H}\alpha}$ or $^3J_{\text{H}\alpha\text{-H}\beta}$ coupling constants measured from 2QF-COSY or COSY-35 spectra, respectively, processed to high digital resolution in F_2 [49]. Hydrogen bond restraints were not employed at any stage of the calculation process. 100 initial structures were calculated using the hybrid distance geometry/simulated annealing program DGII [22]. 80 of the initial structures were further refined by restrained molecular dynamics using the SANDER module of the AMBER all-atom force field v 6.0 [57,58]. Restraints were also included to minimize the difference between observed and calculated ^{1}H chemical shifts for α-protons and for protons of side chains that adopted a fixed χ_1 rotamer [5]. 20 conformations of lowest restraint violation energy were chosen to represent the solution conformations. The program SHIFTS (v 4.0) was used to calculate chemical shifts for a given set of molecular coordinates [62]. The inter-strand twist, Θ, was calculated as described previously [56]. Although this parameter is often measured between non-sequential C^α, throughout this work we have chosen to calculate Θ between adjacent residues since the twist is often not uniformly distributed along the strands [41].

3. Optimization of strand sites

Inspection of structures in the protein database revealed that disulfide bonds can form between adjacent antiparallel strands of a β-sheet provided the backbone atoms of the residues are not hydrogen-bonded to each other (the so called non-hydrogen-bonding or NHB site; Fig. 1) [19,23,53,60]. Moreover, the residues two before or two after the cysteines are often hydrophobic in nature and pack against the disulfide [10]. This suggested to us that a stable β-hairpin scaffold might be developed by including cysteine residues at terminal NHB sites to tether the ends of the peptide, and that including hydrophobic residues at the adjacent NHB sites to pack against the disulfide might nucleate strand formation. This was done in the context of a 10-residue peptide with cysteine residues at position 1 and 10, threonine residues at position 2 and 9 (this amino acid tends to favor an extended backbone [35,51]), and a Glu–Gly–Asn–Lys sequence for residues 4–7 as it should have a moderate tendency to form a type II′ reverse turn [24]. Position 8 was initially chosen to be leucine, and naturally-occurring amino acids were substituted at

Table 1
Comparison of sequences, C_{eff}, $\Delta\Delta G$ and NMR parameters for disulfide cyclized peptides

	Name	Sequence[a]	C_{eff}[b] (mM)	$\Delta\Delta G_{\text{vs bhpW}}$[c] (kcal mol^{-1})	$J > 8$[d]	Cys1[e] (ppm)	Cys10[e] (ppm)
A	bhpW	Ac-CTWE GN KLTC	210	0.0	7	5.20	5.00
	bhpY	Ac-CTYE GN KLTC	98	−0.44	7	5.07	4.91
	bhpF	Ac-CTFE GN KLTC	88	−0.51	5	5.07	4.92
	bhpL	Ac-CTLE GN KLTC	85	−0.53	6	5.04	4.89
	bhpV	Ac-CTVE GN KLTC	73	−0.62	4	4.97	4.85
	bhpK	Ac-CTKE GN KLTC	52	−0.81	3	4.92	4.82
	bhpN	Ac-CTNE GN KLTC	51	−0.83	3	4.84	4.76
B	bhpW	Ac-CTWE GN KLTC	210 ± 4	0.0	7	5.20	5.00
	bhpLW	Ac-CTLE GN KWTC	192	−0.05	7	5.19	5.00
	bhpWW	Ac-CTWE GN KWTC	721	0.72	7	5.35	5.16
C	bhpW	Ac-CTWE GN KLTC	210 ± 4	0.0	7	5.20	5.00
	bhpTV	Ac-CTWE GN KLVC	677	0.68	7	5.30	5.07
	bhpVT	Ac-CVWE GN KLTC	305	0.22	7	5.13	5.01
D	bhpW	Ac-CTWE GN KLTC	210 ± 4	0.0	7	5.20	5.00
	bhpNG	Ac-CTWE NG KLTC	754 ± 12	0.75	6	5.27	5.06
	bhppG	Ac-CTWE pG KLTC	1590 ± 50	1.18	n.d	n.d	n.d
	bhppN	Ac-CTWE pN KLTC	1730 ± 10	1.22	8	5.24	5.03
E	bhpW	Ac-CTWE GN KLTC	210 ± 4	0.0	7	5.20	5.00
	bhpPDG	Ac-CTWE PDG KLTC	167 ± 10	−0.13	5	5.12	4.97
	bhpSDG	Ac-CTWE SDG KLTC	136 ± 10	−0.25	4	5.06	4.94
	bhpSDN	Ac-CTWE SDN KLTC	58 ± 1	−0.75	3	4.84	4.74
	bhpPDN	Ac-CTWE PDN KLTC	38 ± 1	−1.00	3	4.81	4.76
F	bhpW-KS	KCTWE GN KLTCS	273 ± 2	0.15	7	5.20	5.00
	cd1	KCGNQ GS FLTCS	45 ± 4	−0.90	0	4.80	4.72
	cd2	KCTWQ GS FLTCS	120 ± 1	−0.33	6	5.36	5.14
G	bhpW	Ac-CTWE GN KLTC	210 ± 4	0.00	7	5.20	5.00
	emp18*trn*	TYSCHFG PL TWVCKPQ	n.d.	n.d.	4	4.75	4.88
	emp18*cis*	TYSCHFG PL TWVCKPQ	n.d.	n.d.	6	5.52	5.36
	emp18TG	TYSCHFG PL **G**WVCKPQ	>2000	>1.3	7	5.62	5.36
	epo3	SCHFG PL **G**WVCK	896	0.85	6	5.49	5.19
	epo4	SC**RA**G PL **Q**W**L**CK	47	−0.87	1	4.79	4.59
	IGE06	NLPRCTEG PW GWCVM	n.d.	n.d.	5	5.70	5.46

[a]With the exception of IGE06, all peptides contain a C-terminal amide group; spaces separate strand and turn residues.
[b]Errors in C_{eff} are of the order of 5%, which corresponds to a difference in $\Delta\Delta G$ of ∼30 cal mol^{-1}.
[c]$\Delta\Delta G$ values are calculated relative to bhpW at 293 K; positive values indicate a peptide of greater stability.
[d]Number of strand residues with $^3J_{\text{HN-H}\alpha} > 8.0$ Hz; maximum value is 8.
[e]Random coil value for this nucleus is 4.70 ppm.

Table 2
Sequences and thermodynamic parameters for the tryptophan zipper peptides

Peptide	Sequence[b]	T_m K	$\Delta G_{unfold,\ 298\ K}$ kcal mol^{-1}	ΔH_m kcal mol^{-1}	ΔS_m cal mol^{-1}K^{-1}	ΔC_p cal mol^{-1}K^{-1}
trpzip1	SWTW EGNK WTWK	323.0 ± 0.3	0.92	10.8 ± 0.1	33.4	231.4 ± 0.04
gb1[a]	GEWTY DDATKT FTVTE	$\sim$	-0.6	n.d.	n.d.	n.d.
trpzip4	GEWT**W** DDATKT **W**T**W**TE	343.1 ± 0.1	1.69	21.86 ± 0.06	63.7	380 ± 4
trpzip5	GEWTY DDATKT FT**W**TE	315.8 ± 0.2	0.57	13.3 ± 0.1	42.2	325 ± 10
trpzip6	GEWT**W** DDATKT **W**TVTE	317.7 ± 0.5	0.49	10.3 ± 0.3	32.4	236 ± 17

[a]Residues 41–56; $\Delta\Delta G$ estimated assuming additivity of data for trpzip4, 5 and 6.
[b]Spaces separate strand from turn residues; substitutions in the gb1 C-terminal peptide are indicated bold and underlined.

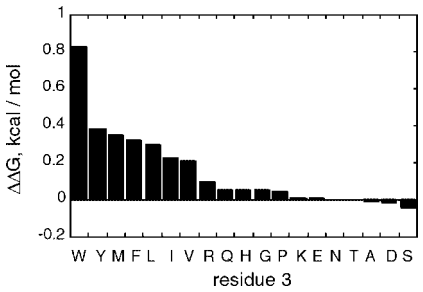

Fig. 2. Folding free energies for X3L8 peptides. The free energies were calculated relative to the peptide with a threonine in position three: $-RT\ln\{C^{X}_{eff}/C^{T}_{eff}\}$; a positive value indicates a more stable peptide.

position 3 (the X3L8-series), with the aim of identifying the residue that most stabilized the β-hairpin structure [10].

The folding free energies of the X3L8 series, determined from the thiol effective concentration measurements, are shown in Fig. 2. Hydrophobic residues, especially those with aromatic rings, are found to be stabilizing, with tryptophan being the best (the importance of cross-strand hydrophobic interactions has been hinted at in previous studies of β-hairpins [3,31,39,47]). The trend observed in Fig. 2 does not correlate with previously published scales of β-strand propensity based on substitutions into guest sites within β-sheets of proteins [34,35,51]. In these scales, threonine is usually the most favored residue type, whereas in our model hairpin system, threonine is not stabilizing and inclusion of tryptophan stabilizes the β-hairpin by $\sim$0.8 kcal mol^{-1} relative to threonine. The differences in the scales presumably result from the host system used to measure the stabilizing effects. In protein host-guest studies, the requirements of forming an entire β-sheet, and the possibility of stabilizing interactions between the sheet and the rest of the protein, may obscure the underlying trends in strand–strand stabilization. However, in the isolated hairpin case there are no extended tertiary interactions, and large hydrophobic side chains are clearly able to make the most stabilizing interactions with the opposite strand.

A qualitative assessment of the degree of folding in the oxidized state was made for a number of the X3L8 peptides using ^{1}H NMR. Deviations of H$^{\alpha}$ chemical shift from their random coil values (so-called secondary chemical shifts), the presence of strand residues with $^3J_{HN\text{-}H\alpha} > 8.0$ Hz, and the observation of nuclear Overhauser effects between protons in the different strands are all indicative of the formation of extended polypeptides and their association to form a β-hairpin. The trend observed in the magnitude of these parameters does correlate with the free energy of folding (Table 1) derived from the disulfide

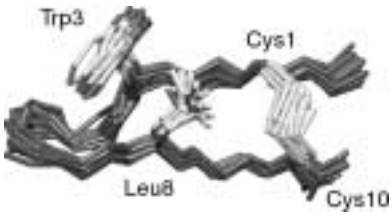

Fig. 3. Ensemble of 20 structures calculated for bhpW (mean rms to the mean structure = 0.39 ± 0.09 Å for N, C^{α} and C atoms). The side chains off the four NHB residues are depicted and labeled.

exchange equilibrium measurements, and suggests that the latter are reflective of the degree of folding in the oxidized state.

The peptide with tryptophan at position 3 (bhpW) was studied in more detail by ^{1}H NMR. As described in the Materials and methods section, 79 inter-proton distance restraints, 10 backbone ϕ dihedral angle restraints and 5 side chain $\chi 1$ restraints were generated from this analysis. Moreover, the chemical shifts also provide sensitive indicators of structure that can provide additional experimental restraints [13] to guide the structure calculation process [5]. The final structures calculated for bhpW are well-defined at the backbone level (mean RMSD to the mean structure of 0.39 ± 0.08 Å) and are depicted in Fig. 3. The peptide adopts the designed fold, with the two strands (Cys1–Thr2–Trp3–Glu4 and Lys7–Leu8–Thr9–Cys10) in an antiparallel arrangement connected by a type II′ reversed turn (Gly5–Asn6). Four hydrogen bonds are present connecting the strands, and the cysteine side chains adopt the conformation observed for disulfide bonds between adjacent antiparallel strands in proteins ($\chi 1 = -60°$, $\chi 2 = -90°$; $\chi 3 = +100°$; $\chi 4 = -90°$; $\chi 5 = -60°$ [53]). The two pairs of NHB side chains (Cys1–Cys10 and Trp3–Leu8) form a cluster on one side of the hairpin. Although the observed values of $^{3}J_{\mathrm{H}\alpha\text{-}\mathrm{H}\beta}$ for Trp3 and Leu8 suggest that more than one χ_1 rotamer is being sampled in solution, a single rotamer is observed in the ensemble suggesting that these side chains are being "pinned" by the observed ROE restraints [21].

As with β-sheets in proteins, the strands of bhpW twist around each other in a right-handed sense. The inter-strand twist is moderate next to the disulfide ($\Theta = 18°$ for the C^{α} of Cys1, Cys10–Thr2, Thr9) and much more pronounced on either side of the NHB hydrophobic residues ($\Theta 29°$ for the C^{α} of Thr2, Thr9–Trp3, Leu8 and 31° for the C^{α} of Trp3, Leu8–Glu4, Lys7). This degree of twist is higher than the optimal value of 20–25° estimated from molecular mechanics calculations [56], but is not beyond the range of values observed in proteins [63]. However, twists of this magnitude are usually only observed in isolated β-hairpins or edge strands of β-sheets, not in the interior strands of extended β-sheets [63]. Indeed, Richardson et al. have postulated that twisting of edge strands is one mechanism by which β-sheet proteins avoid self-association via the formation of extended intermolecular edge–edge contacts [40]; this might also explain the absence of aggregation observed for our twisted β-hairpin peptides. Within each strand, the twisting is localized to the N-terminal side of the NHB hydrophobic residues, as judged by the sum of backbone dihedral angles between adjacent $C^{\alpha}(\psi^{i} + \phi^{i+1})$ [41]. The non-uniform twisting of each strand is reflected in the NMR parameters: the backbone coupling constant $^{3}J_{\mathrm{HN}\text{-}\mathrm{H}\alpha}$ of Trp3 and Leu8 are 8.4 and 7.8 Hz, respectively (lower than the expected value of 8.5–10 Hz for an extended strand), and the $^{13}C^{\alpha}$ secondary chemical shifts are close to zero (compared to ~ -2.0 ppm in regular extended strands [43,52]).

Having identified the optimal residue at position 3 in our β-hairpin scaffold, we next made substitutions at position 8 (originally leucine) with a leucine fixed at position 3 (L3X8 series) [42]. Due to the twist of the strands, position 3 and 8 are not geometrically equivalent: the side chain of residue 3 is

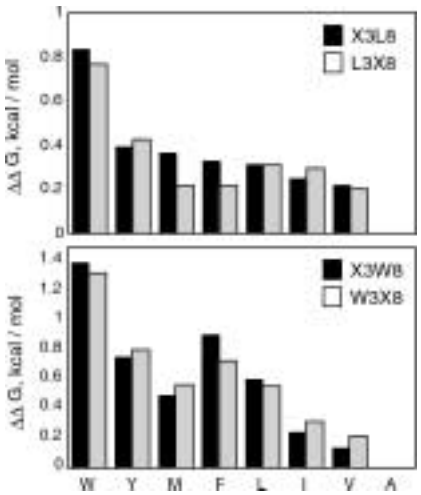

Fig. 4. (Top) Comparison of folding free energies for X3L8 and L3X8 series of peptides. (Bottom) Comparison of folding free energies for X3W8 and W3X8 series of peptides. All energies are with respect to the peptide with alanine at the variable site.

closer to the turn whilst the side chain of residue 8 is closer to the disulfide. In spite of this geometric difference, substitutions at position 8 are energetically very similar to those at position 3 (Fig. 4(top)), with tryptophan conferring the greatest stability. Families of peptides were also studied with position 3 or 8 fixed at tryptophan (the W3X8 and X3W8 series). Once again, the trend in C_{eff} is the same in both families (Fig. 4(bottom)), suggesting that the two NHB sites are equivalent and that neither makes specific, packing interactions with the disulfide or the turn region (this is in contrast to some recent reports that specific "diagonal" cross-strand residue pairs can be stabilizing [54]). A more detailed analysis of the data in Fig. 4 indicates that linear free-energy relationships exist between the different families of peptides [42]. Interestingly, the free-energy relationships between Trp and Leu have non-unit gradients; substitutions opposite tryptophan are always ∼2.5-fold more stabilizing than opposite leucine and there are no residue pair-specific interactions between position 3 and 8 that are especially stabilizing. We hypothesize that the enhanced stability of tryptophan arises from interactions with the backbone of the opposite strand; from the backbone twist point of view, position 3 and 8 are equivalent, providing an explanation for the energetic equivalence of substitutions at these sites.

Due to the independence of the two sites, the most stable β-hairpin peptide is found with tryptophan residues at position 3 and 8; this peptide is over 1.2 kcal mol^{-1} more stable than the peptide with leucine residues at both sites. The ^{1}H NMR parameters for this peptide (bhpWW) indicate that it is well-folded at the backbone level (Table 1). Interestingly, the CD spectrum of bhpWW contains two intense exciton-coupled bands (a negative one at 215 nm and a positive one at 229 nm) that are indicative of an interaction between two proximal aromatic chromophores [18]. In spite of this Trp3–Trp8 interaction, the $^3J_{\text{H}\alpha\text{-H}\beta 2}$ and $^3J_{\text{H}\alpha\text{-H}\beta 3}$ coupling constants for both tryptophan side chains are ∼7.5 Hz, indicating that χ_1 values of -60° and 180° are sampled with approximately equal frequency. Initial structure calculations confirmed that a single conformation could not satisfy all of the observed ROEs to the tryptophan ring protons. Instead, four separate ensembles of structures were determined with χ_1 set to -60° or 180° for Trp3 and Trp8 (Fig. 5). For each calculation, tryptophan ring ROEs that were not consistent with the particular χ_1 values were manually removed, although all ROEs were utilized in at least one of the calculations. Although the tryptophan side chain orientations differ between the ensembles, the backbone geometry, including the type II′ turn, cross-strand hydrogen bonds and right-handed twist of the strands, is similar.

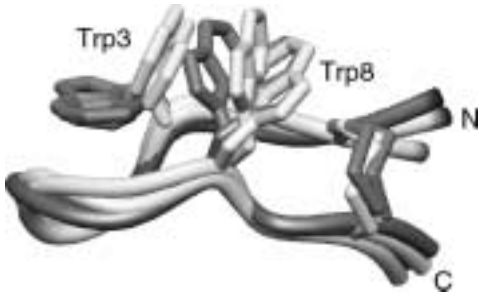

Fig. 5. Minimized mean structures from the four ensembles calculated for bhpWW. The two structures with χ_1 for Trp3 of -60° are shown in the lighter shading.

These results indicate that the solution conformation of bhpWW is best represented as some mixture of the four individual conformations, since only then can all of the NMR data be explained.

Our most recent work has focussed on stabilizing our CX_8C scaffold by substitutions at the HB sites 2 and 9 (initially fixed at threonine residues) [41]. In contrast to the NHB sites, substitutions at position 2 and 9 are not energetically equivalent. Hydrophobic β-branched amino acids are very stabilizing at position 9 (by $\sim$0.7 kcal mol^{-1}) compared to threonine, but only slightly stabilizing (by $\sim$0.2 kcal mol^{-1}) at position 2 [41]. We attribute this energetic asymmetry to the asymmetric nature of the strand twisting (both cysteine residues are less twisted and both NHB residues are more twisted): presumably, the particular environment surrounding position 9 is much more compatible with a valine or isoleucine side chain than the environment surrounding position 2. The stabilization achieved by position 9 substitutions is independent of the residues at the NHB sites. Thus, stabilizing features at several sites may be combined to form a much more stable scaffold. The most stable frameworks will be able to induce a β-hairpin conformation for a much larger proportion of turn sequences, thereby enhancing the utility of our scaffold for mimicking hairpin loops in proteins (see below).

4. Turn residues

We next investigated the influence that the turn residues had on the stability of the disulfide cyclized β-hairpin system [10]. In addition to the original GN turn, the turn sequences NG, pN and pG were also studied ("p" indicates a proline of D stereochemistry at the α-carbon). For each turn sequence, C_{eff} was measured for several members of the X3L8 series. For all three turns, the rank ordering of stability is the same as in the original GN-turn series, with the Trp3 peptides being most stable. Free energy relationships derived from these data indicate that the turn and strand residue 3 make independent contributions to the stability of the hairpin. The additivity of the C_{eff} data also allow the relative stability of the different turn types to be evaluated: substituting GN for NG leads to a $\sim$0.7 kcal mol^{-1} increase in stability, whilst the D-proline turns are even more stabilizing ($\sim$1.2 kcal mol^{-1} for pN and pG). Structures calculated for these peptides on the basis of the NMR data demonstrated that the scaffold observed in bhpW was preserved, although the turn type and orientation with respect to the strands differed [10]. We note [10], as have others [20,30,59], that a stable β-hairpin with a tight, 2-residue turn will only be populated if a type-I$'$ or type-II$'$ turn can form. This results from the compatibility of the natural right-handed twist of the strands ($\Theta \sim 25^\circ$) and the inherent twist of a primed turn ($\Theta \sim 25^\circ$ for I$'$ and $\sim 15^\circ$ for II$'$). In contrast, an unprimed turn has a negative Θ that cannot readily connect a pair of antiparallel strands;

indeed, for this reason early attempts to form hairpins with proline-induced type I turns lead to the formation of bulged three-residue turns with mis-registered strands [12].

The sequences used to connect the strands described above have a moderate to high propensity to form turns suitable for the formation of a β-hairpin. We next wanted to test the ability of the bhpW scaffold to stabilize less stable turn sequences present in hairpin loops of proteins. Given the linear free energy relationships described above, the fraction of molecules folded into the desired hairpin conformation will be a balance between the relative energies of turn and of the strand interactions. The first example we chose was the C′–C″ hairpin loop from the T-cell surface protein CD4 (residues 37–46) [10]. The human immunodeficiency virus uses this cell-surface protein as a co-receptor for gaining entry into cells via association with the virus coat protein gp120. A co-crystal structure of CD4 protein bound to gp120 suggests that the 37–46 hairpin loop contributes 63% of the buried surface of CD4, with much of this coming from the side chain of Phe43 [26]. Thus, peptides that mimic this portion of CD4 might provide useful starting points from which antagonists of the gp120–CD4 interaction might be developed [55].

The initial peptide based on the C′–C″ loop containing the sequence of CD4 residues 38–45 with terminal cysteine residues (cd1; Table 1) had a very low C_{eff}, and NMR data concurred that it was not a well-folded hairpin [10]. Although the sequence of the C-terminal strand is appropriate (Leu–Thr), the N-terminal strand residues Gly–Asn are not favorable for hairpin formation (e.g., an asparagine at the NHB site is not stabilizing, see Fig. 2). In peptide cd2, the residues from bhpW were substituted into the N-terminal strand. We reasoned that in the co-crystal structure, these side chains of CD4 are orientated away from the gp120 surface [26], hence the presence of Thr–Trp should not interfere sterically with binding by the peptide. Structures calculated on the basis of the NMR data for cd2 show it to be well-ordered with a type II′ turn connecting strands with hydrophobic packing of NHB and cysteine residues along one face (Fig. 6). However, C_{eff} measurements suggest that the QGSF turn destabilizes the folding free energy by 0.5 kcal mol^{-1} relative to bhpW. The structure determined for cd2 is quite similar to the corresponding loop of CD4 (RMSD of 0.93 Å for N, C$^{\alpha}$ and C atoms of residues 37–46; Fig. 6). The observed values of $^{3}J_{\text{H}\alpha\text{-H}\beta}$ for Phe7 (Phe43 in CD4) suggest that the single rotamer observed in the peptides is an artifact, and that this side chain probably samples several conformations, including the one observed in the gp120 co-crystal. In spite of the structural similarity between cd2 and the C′–C″ loop of CD4, we have not been able to observe binding of cd2 to gp120 ($IC_{50} \gg 1$ mM). This suggests that although the C'–C″ hairpin loop is necessary for binding to gp120, it is not sufficient, and that other binding determinants are necessary for recognition of gp120 [10].

Loops connecting hairpin strands in proteins are often more complex than the simple I′ or II′ two-residue turns studied thus far with our model hairpin system [45]. We next chose to study turns with 3 residues that are commonly found in proteins as type I turns with a β-bulge [4]. The GN turn in bhpW was replaced with several three-residue turns that have been observed in protein structures; a number of single amino acid changes were made within these turns to assess the effect on stability of individual side chains. The three-residue turns all resulted in hairpins of lower stability (C_{eff}) than bhpW, with the destabilization ranging from 0.13 to $>$1.0 kcal mol^{-1}. Structures calculated for the most stable peptide (PDG) indicate that the scaffold conformation is preserved while the Pro–Asp forms a type I reverse turn, and the glycine forms a β-bulge with a positive ϕ (Fig. 7). This conformation is very similar to that seen in several proteins that contain a β-hairpin connected by a PDG turn, for example residues 306–308 of 15-lipoxygenase (Fig. 7(bottom); [17]). Although the three-residue turn peptides span a range of stabilities, the pattern of backbone chemical shifts (H$^{\alpha}$, C$^{\alpha}$ and C$^{\beta}$) [43] and sequential H$^{\text{N}}$–H$^{\text{N}}$ ROEs [61] in the turn are consistent with the type-I turn + β-bulge being the dominant conformation in every case. Thus, the C_{eff} measurements are reporting directly on the relative stability of this turn type for a particular

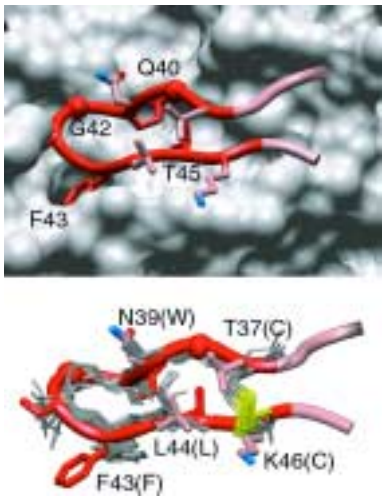

Fig. 6. (Top) C′–C″ hairpin loop of CD4 binding to gp120. The C′–C″ loop of CD4 is shown in tube format (the rest of CD4 is removed for clarity), whilst gp120 is shown as a solvent-accessible surface; side chains that make prominent contact with gp120 are labeled. (Bottom) Comparison of cd2 to the C′–C″ loop conformation in the CD4-gp120 complex. Labels correspond to the residue in CD4; letters in parentheses indicate the residue type in cd2. Note that although the calculated structures have the Phe side chain of the peptide in an orientation different from that in the CD4-gp120 complex, the NMR data indicate that it actually samples several orientations in solution, including that present in the co-crystal structure.

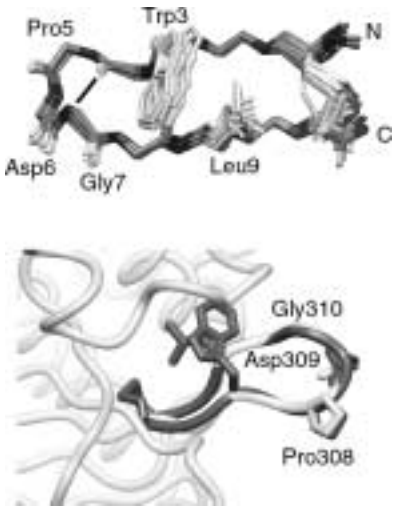

Fig. 7. (Top) Ensemble of 20 structures determined for bhpPDG; the hydrogen bond within the type I reverse turn is indicated by the black line. (Bottom) Comparison of representative bhpPDG structure (grey) with the PDG-containing loop from 15-lipoxygenase (white).

sequence. Single residue substitutions within the three-residue turns reveal a context-dependence to the associated changes in free energy (Table 1). This implies single-residue turn potentials determined from statistical analysis of amino acid preferences in protein structures may not be relevant in all cases [24].

5. β-hairpin erythropoietin agonist peptides

During the development of our β-hairpin scaffold, several peptides discovered from phage display libraries have been reported that are able to bind to and affect the activity of a number of proteins [46]. Interestingly, two of these peptides contain a CX_8C motif and in the bound state adopt a β-hairpin conformation with a tryptophan at the C-terminal NHB site within the cycle. Since the β-hairpin conformation is necessary for protein binding in both cases [28,37], the selection of tryptophan offers an entropic benefit to binding by its ability to pre-organize the β-hairpin prior to association with protein. In the case of the FcεRIα-binding peptide IGE06, the β-hairpin conformation is highly populated in the free peptide [37]. Although the peptide EMP-1 adopts a β-hairpin conformation when bound to the erythropoietin receptor (EPO-R) [28], the structure of the peptide in the absence of binding protein has not been reported.

We chose to investigate the conformational behavior of the EPO-R antagonist peptides in solution. ^{1}H NMR spectra revealed that EMP-18 (the shortest EPO-R-binding peptide that still exhibits agonistic activity [25]; see Table 1 for sequence) is conformationally heterogeneous in solution, with two sets of resonances present in a 3 : 2 ratio. The resonances could be assigned for both species, and inspection of the sequential NOEs revealed that the most populous form had a *trans* Gly8–Pro9 peptide bond, whilst the less populated species had the *cis* orientation. Although some cross-strand NOEs are observed for the *trans* isomer in the vicinity of the cysteine residues, the remaining NMR parameters are not indicative of a well-folded β-hairpin conformation [50]. However, in the *cis* isoform, cross-strand NOEs, $^3J_{\text{HN-H}\alpha}$ and H^α secondary chemical shifts are all consistent with the formation of a β-hairpin [50]. Structures calculated for this isoform have phenylalanine and tryptophan residues occupying the NHB sites in proximity to the cysteine side chains, whilst a Pro-Leu type I turn connects the strands (Fig. 8(top)). Thus, although the type-I turn enforced by the proline cannot be accommodated in a stable β-hairpin due to its incorrect twist, flipping the peptide bond preceding the proline is sufficient to alter the twist of the turn ($\Theta \sim 30^\circ$) and allow the β-hairpin to form.

Inspection of the sequence for the IgE-receptor antagonist peptide (IGE06) indicated that even though it has a proline at the turn $i+1$ position (and hence a type I turn), it is still able to adopt a stable β-hairpin conformation by virtue of having a glycine with a positive ϕ at the turn $i+3$ position [37]. When this turn $i+3$ glycine substitution was made in the context of EMP-18, or in a truncated version (epo3), one predominant species resulted in solution (Gly–Pro bond $>$ 90% *trans*) that contained a well-formed β-hairpin (Fig. 8(middle); Fig. 9(top)). Further, we hypothesized that the enhanced conformational preference of emp18(T10G) might allow it to bind to EPO-R more tightly. However, we have been unable to demonstrate any interaction with EPO-R (agonistic or antagonistic). A comparison of the structure of epo3 with that of peptide in the EPO-R-bound state indicates that although the strand regions of the peptides overlay well, the relative orientation of the turn is affected by the positive ϕ of Gly at the turn $i+3$ position (Fig. 8(bottom)). In the co-crystal structure with EPO-R, there are important intermolecular hydrophobic interactions with the strand residues and three intermolecular hydrogen bonds to backbone carbonyl groups in the turn. We speculate that the combination of these interactions is able to overcome the strain of connecting β-hairpin strands with a type I turn (as is observed in the co-crystal structure) and maintain tight binding, whereas in EMP18(T10G) the incorrect orientation of strands and turn preclude a stable interaction with EPO-R.

A phage library similar to that used to discover the EPO-R antagonists was used recently to identify antagonists of the interaction between insulin-like growth factor-I (IGF-I) and IGF binding protein-1 (IGFBP-1) [29]. Interestingly, although 6 of 10 residues within the disulfide cycle are identical with

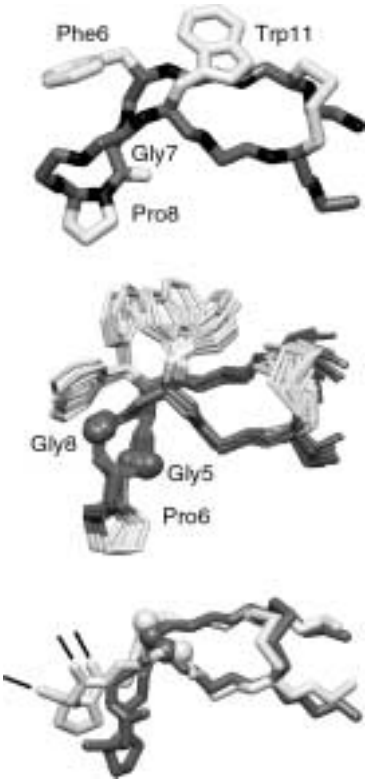

Fig. 8. (Top) minimized mean structure of EMP-18 with a *cis* Gly–Pro peptide bond. Note that Phe6 and trp11 both sample more than one side chain orientation. (Middle) Ensemble of 20 structure for epo-3. (Bottom) Structural comparison of epo-3 (grey) and EMP-1 in the EPO-R-bound state (white) overlaid on the backbone atoms of the strand residues; the black lines indicate those carbonyls of EMP-1 that form inter-molecular hydrogen bonds to EPO-R.

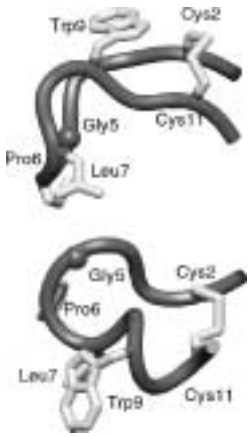

Fig. 9. (Top) Representative structure of epo-3. (Bottom) Representative structure of epo-4. The six common side chains within the disulfide cycles of epo-3 and epo-4 are labeled. The structures are depicted with their disulfide bonds in similar orientations.

EMP-18, the IGFBP-1 antagonist peptide adopts a completely different conformation and contains an N-terminal loop and a C-terminal helix. A truncated 12-residue version of the IGFBP-1 antagonist (epo4; Fig. 9; see Table 1 for sequence) has a 66% sequence identity to the β-hairpin epo3, yet is also helical at its C-terminus. We have studied all 16 hybrid peptides of epo3/epo4 in order to evaluate which of the 4 amino acid differences control the selection of β-hairpin vs. α-helical conformation [50]. Spectroscopic methods (NMR and CD) along with C_{eff} measurements were used to assess the type and extent of folding in each case. The residue at position 8 was most discriminating due to its location at the turn $i + 3$ site: peptides with Gly8 were either β-hairpins or unfolded, whereas peptides with Gln8 were either α-helical or unfolded. Within the Gly8-containing peptides, the order of importance for maintaining the β-hairpin conformation was found to be Phe4Ala $>$ Val10Leu $>$ His3Arg. The preference for Phe is expected from the studies described above (Fig. 2) since this residue is at the NHB site. Likewise, the preference for a valine preceding the second cysteine is apparent in our studies with bhpW (Table 1). Thus, the phage selection process seems to have selected residues that not only recognize EPO-R but also predispose the peptide to adopt a β-hairpin conformation. Moreover, these observations suggest that the construction of phage display libraries in which some residues are fixed so as to favor formation of a β-hairpin might generate novel ligands that have a predefined conformational preference, thereby simplifying subsequent structure–function analysis.

6. Tryptophan zippers

The studies described above indicate that the stabilization of a β-hairpin by inclusion of tryptophan residues at a NHB site is independent of turn type and cross-strand NHB residue. We hypothesized that we could extend this by replacing the cysteine residues at the terminal NHB site with tryptophan to produce a linear peptide that adopts a stable β-hairpin conformation [9]. A peptide based on this four-tryptophan scaffold (tryptophan zipper; trpzip1) with an EGNK turn sequence was characterized by NMR and found to be highly folded at 15°C in aqueous solution (Table 2). All the hallmarks of a well-folded β-hairpin were present, including numerous and substantial deviations of ^{1}H chemical shifts from random coil values (some by more than 2.0 ppm), numerous cross-strand NOEs and backbone $^3J_{\text{HN-H}\alpha}$ coupling constants $>$8.0 Hz. In spite of the presence of four tryptophan residues in a 12-residue peptide, line widths of the NMR resonances and analytical ultracentrifugation data all point to the monomeric nature of the tryptophan zipper peptides (i.e., folding is not dependent on oligomerization) [9]. The trpzip1 is also well-folded from the side chain point of view: $^3J_{\text{H}\alpha\text{-H}\beta}$ indicate that all four tryptophan residues adopt a fixed χ_1 and numerous NOEs are observed between the rings. Structure determination for trpzip1 reveals the nature of the β-hairpin: the type II′ turn connects two antiparallel strands with the two terminal and the two central tryptophan side chains packed in a well-defined edge-to-face fashion (note that initial structure determinations had face-to-face packing between each pair of aromatic rings [9]; subsequent quantitative analysis of ^{1}H chemical shifts indicate that these data are best described by changing χ_1 and χ_2 of the outer tryptophan residues to produce the edge-to-face packing shown in Fig. 10(top); [8]). The strands of trpzip1 have a pronounced twist, with the majority of this occurring on the N-terminal side of each tryptophan residue; in spite of the twist, all of the expected cross-strand hydrogen bonds are present.

As was seen with bhpWW, the inter-strand tryptophan pairing gives rise to intense exciton coupled bands in the CD spectrum of the tryptophan zipper peptides. Note that these bands are much more intense than the usual CD signature of β-structure [31,39] and can provide a very sensitive measure of the extent of folding. Monitoring the CD intensity at 229 nm as a function of temperature indicates that the

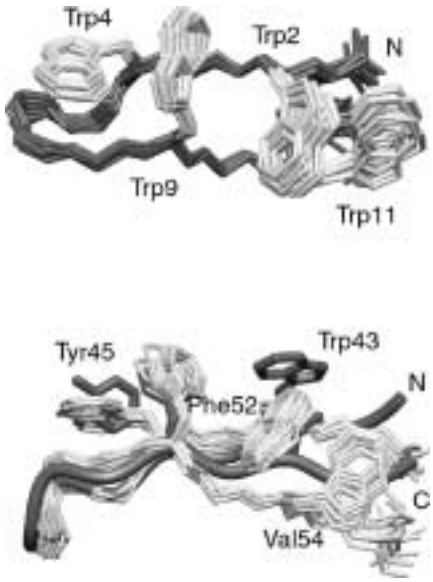

Fig. 10. (Top) Ensemble of 20 structures of trpzip1; for clarity, only the side chains of the four tryptophan residues are shown and labeled. (Bottom) Overlay of trpzip4 (white) with the C-terminal β-hairpin from the protein G B1 domain (grey) using backbone atoms of residues 46–52 of GB1 (rmsd = 0.65 Å). For clarity, only the side chain atoms of the four NHB hydrophobic residues are depicted.

unfolding event is cooperative, reversible and independent of peptide concentration. The thermodynamic parameters for this event are obtained by appropriate fitting to the denaturation curve (Table 2): trpzip1 unfolds with a T_{m} of 323 K; at ambient temperature trpzip1 folds via an enthalpically driven process and is >80% folded. On a per-residue basis, the parameters in Table 2 are comparable to the values observed in larger proteins [1,2]. Moreover, the data are also best fit by allowing a non-zero value for the change in heat capacity (ΔC_{p}), a feature that is also observed in cooperative folding of proteins. Thus, from a structural and thermodynamic point of view, the tryptophan zipper molecules conform to traditionally accepted views of protein behavior, and may be considered as true "mini-proteins" [13].

The 16 C-terminal residues from the B1 IgG-binding domain of protein G have been used previously as a model for the formation of β-hairpin structure by a linear peptide [3]. In the folded, intact B1 domain, the C-terminus forms a β-hairpin with four hydrophobic residues at NHB sites (W43, Y45, F52 and V54) that pack into the core of the protein. This motif has been proposed as a nucleator of hairpin structure [36], although the native peptide [3], or a variant with a high-propensity type I′ pG turn [14], exhibit marginal stability at room temperature. We chose to replace the three non-tryptophan NHB residues of the gb1 peptide with tryptophan (trpzip4; [9]). This peptide is exceptionally stable, as judged by both CD thermal melts ($T_{\mathrm{m}} = 343$ K; Table 2) and NMR data [9]. We estimate that each pair of cross-strand tryptophan residues contribute $\sim$1 kcal mol^{-1} to the free energy of folding of the hairpin relative to the wild-type residue pairs, making the tryptophan zipper variant far more stable than the wild-type hairpin (>95% folded at 293 K vs. $\sim$30% folded for the wild-type). Overall, the structure determined for trpzip4 is quite similar to the equivalent hairpin in the intact B1 domain (Fig. 10(bottom)), especially in the turn region (RMSD = 0.65 Å for residues 46–52), with the turn conformations being very similar. However, in keeping with our other hairpin scaffolds, the strands of trpzip4 are quite twisted ($\Theta \sim 30^\circ$ per residue) compared to the hairpin in the intact protein ($\Theta \sim 10^\circ$ per residue).

7. Conclusions

Through the development of a disulfide-cyclized model system, we have been able to understand some of the factors that stabilize β-hairpin conformations. The presence of the disulfide at the appropriate strand location not only stabilizes the fold, but also affords a sensitive measure of the relative free-energies of folding for our peptides. A systematic investigation into the effect of residue type at the non-hydrogen-bonded sites within this peptide revealed that hydrophobic residues, especially tryptophan, are especially stabilizing [8]. The two non-hydrogen-bonded sites are found to be energetically equivalent (in spite of the hairpin twist making them structurally distinct) and to participate in positively cooperative strand interactions [42]. Interestingly, the cooperativity is not associated with particular pairs of side chains; placement of the stabilizing tryptophan at one site improves the stabilizing effect of *all* substitutions in the other strand by ∼2.5-fold. In contrast, the stabilizing effect of substitutions in the 2-residue turn was found to be independent of residues in the strands [8]. Thus, our model hairpin appears to be modular and optimization of strand and turn portions may be conducted independently.

We have used NMR spectroscopy to characterize many of our β-hairpin peptides. Not only does NMR provide evidence for the folded nature of the peptides (and even a semi-quantitative evaluation of the degree of folding), but it can also give insights into the presence of internal motions of backbone or side chain atoms. In the case of well-folded peptides, the NMR data may also be used to determine three-dimensional structures, thereby allowing a correlation of stabilizing substitutions with conformational features [8]. Pairs of cross-strand tryptophan residues are not only very stabilizing to our CX_8C scaffold, but their interaction also gives rise to a pair of intense bands in the CD spectrum that are highly indicative of the folded β-hairpin [50]. By combining two pairs of non-hydrogen-bond tryptophan residues, linear peptides have been designed that also adopt a stable β-hairpin fold [9]. The intense CD bands are also observed in these molecules, facilitating characterization of the thermal unfolding process. These peptides, dubbed tryptophan zippers, have thermodynamic and structural characteristics equivalent to full proteins, hence they represent the smallest “mini-protein” domains yet described.

The independence of strand and turn residues indicates that our scaffold will have utility in mimicking hairpin loops from proteins: by using a stable scaffold we should be able to impart a conformational preference to sequences that do not have a strong tendency to adopt turn conformations. We have put this into practice by stabilizing the C′–C″ turn from CD4 in a 12-residue peptide in an attempt to develop antagonists of gp120 binding [8]. The C-terminal hairpin turn from the B1 domain of protein G has also been accurately reproduced, this time in the tryptophan zipper context [9]. Finally, 3-residue turn sequences have also been introduced into the disulfide-linked scaffold, and found to adopt similar conformations to the same turn sequences observed in full-length proteins [4]. Interestingly, several of the sequence elements that stabilize our scaffold have also been observed in protein ligands developed from naïve phage display libraries that also have a tendency to adopt a β-hairpin conformation [37,50]. These two areas of research may be combined to develop peptide libraries on phage in which some residues are fixed to impart a predefined conformation to the randomized portion of the peptide.

Acknowledgements

We thank: Joshua Theaker, Ricky Tong and Eleanor Park for their assistance with Ceff measurements, NMR data collection and interpretation for the CX_8C peptides; Dr. Fred de Sauvage for running the EPO-R assays and Drs. Dave Case and Wayne Fairbrother for advice and assistance with incorporating chemical shift refinements in AMBER.

References

[1] P. Alexander, S. Fahnestock, T. Lee, J. Orban and P. Bryan, Thermodynamic analysis of the folding of the streptococcal protein G IgG-binding domains B1 and B2: why small proteins tend to have high denaturation temperatures, *Biochemistry* **31** (1992), 3597–3603.

[2] W.J. Becktel and J.A. Schellman, Protein stability curves, *Biopolymers* **26** (1987), 1859–1877.

[3] F.J. Blanco, G. Rivas and L. Serrano, A short linear peptide that folds into a native stable β-hairpin in aqueous solution, *Nature Struct. Biol.* **1** (1994), 584–590.

[4] T. Blandl, A. Cochran and N.J. Skelton, Turn stability in β-hairpins: 3:5 Type I G1 bulge turns, in press.

[5] D.A. Case, Calibration of ring-current effects in proteins and nucleic acids, *J. Biomolec. NMR* **6** (1995), 341–346.

[6] J. Cavanagh, W.J. Fairbrother, A.G. Palmer and N.J. Skelton, *Protein NMR Spectroscopy, Principles and Practice*, Academic Press, New York, 1995.

[7] A. Chakrabartty and R.L. Baldwin, Stability of α-helices, *Adv. Prot. Chem.* **46** (1995), 141–176.

[8] A.G. Cochran, N.J. Skelton and M.A. Starovasnik, Correction: Tryptophan zippers: stable, monomeric β-hairpins, *Proc. Natl. Acad. Sci. USA* **99** (2002), 9081.

[9] A.G. Cochran, N.J. Skelton and M.A. Starovasnik, Tryptophan zippers: stable, monomeric β-hairpins, *Proc. Natl. Acad. Sci. USA* **98** (2001), 5578–5583.

[10] A.G. Cochran, R.T. Tong, M.A. Starovasnik, E.J. Park, R.S. McDowell, J.E. Theaker and N.J. Skelton, A minimal peptide scaffold for β-turn display: optimizing a strand position in disulfide-cyclized β-hairpins, *J. Am. Chem. Soc.* **123** (2001), 625–632.

[11] C. Das, G.A. Naganagowda, I.L. Karle and P. Balaram, Designed beta-hairpin peptides with defined tight turn stereochemistry, *Biopolymers* **58** (2001), 335–346.

[12] E. de Alba, M.A. Jiménez and M. Rico, Turn residue sequence determines β-hairpin conformation in designed peptides, *J. Am. Chem. Soc.* **119** (1997), 175–183.

[13] W.F. DeGrado, C.M. Summa, V. Pavone, F. Nastri and A. Lombardi, De novo design and structural characterization of proteins and metalloproteins, *Ann. Rev. Biochem.* **68** (1999), 779–819.

[14] J. Espinosa and S. Gellman, A designed β-hairpin containing a natural hydrophobic cluster, *Angew. Chem. Int. Ed.* **39** (2000), 2330–2333.

[15] C. Falcomer, Y. Meinwald, I. Choudhary, S. Talluri, P. Milburn, J. Clardy and H. Scheraga, Chain reversals in model peptides: Studies of cystine-containing peptides. 3. Conformational free energies of cyclization of tetrapeptides of sequence Ac-Cys-Pro-X-Cys-NHMe, *J. Am. Chem. Soc.* **114** (1992), 4036.

[16] S.H. Gellman, Minimal model systems for beta sheet secondary structure in proteins, *Curr. Op. Chem. Biol.* **2** (1998), 717–725.

[17] S. Gillmor, A. Villasenor, R. Fletterick, E. Sigal and M. Browner, The structure of mammalian 15-lipoxygenase reveals similarity to the lipases and the determinants of substrate specificity, *Nature Struct. Biol.* **4** (1997), 1003–1009.

[18] I.B. Grishina and R.W. Woody, Contributions of tryptophan side chains to the circular dichroism of globular proteins: exciton couplets and coupled oscillators, *Faraday Discussions* (1994), 245–262.

[19] K. Gunasekaran, C. Ramakrishnan and P. Balaram, Beta-hairpins in proteins revisited: lessons for de novo design, *Protein Eng.* **10** (1997), 1131–1141.

[20] T.S. Haque and S.H. Gellman, Insights on β-hairpin stability in aqueous solution from peptides with enforced type I′ and type II′ β-turns, *J. Am. Chem. Soc.* **119** (1997), 2303–2304.

[21] T. Havel, The precision of protein structures determined from NMR data: reality or illusion?, in: *Proteins: Structure, Dynamics, Design*, V. Renugopalakrishnan, P.R. Carey, I.C.P. Smith, S.-G. Huansand and A.L. Storer, eds, ESCOM Science Publishers, Leiden, Holland, 1991, pp. 110–115.

[22] T.F. Havel, An evaluation of computational strategies for use in the determination of protein structure from distance constraints obtained by nuclear magnetic resonance, *Prog. Biophys. Mol. Biol.* **56** (1991), 43–78.

[23] E.G. Hutchinson, R.B. Sessions, J.M. Thornton and D.N. Woolfson, Determinants of strand register in antiparallel beta-sheets of proteins, *Protein Sci.* **7** (1998), 2287–2300.

[24] E.G. Hutchinson and J.M. Thornton, A revised set of potentials for β-turn formation in proteins, *Protein Sci.* **3** (1994), 2207–2216.

[25] D.L. Johnson, F.X. Farrell, F.P. Barbone, F.J. McMahon, J. Tullai, K. Hoey, O. Livnah, N.C. Wrighton, S.A. Middleton, D.A. Loughney, E.A. Stura, W.J. Dower, L.S. Mulcahy, I.A. Wilson and L.K. Jolliffe, Identification of a 13 amino acid peptide mimetic of erythropoietin and description of amino acids critical for the mimetic activity of EMP1, *Biochemistry* **37** (1998), 3699–3710.

[26] P.D. Kwong, R. Wyatt, J. Robinson, R.W. Sweet, J. Sodroski and W.A. Hendrickson, Structure of an HIV gp120 envelope glycoprotein in complex with the CD4 receptor and a neutralizing antibody, *Nature* **393** (1998), 648–659.

[27] E. Lacroix, T. Kortemme, M. Lopez de la Paz and L. Serrano, The design of linear peptides that fold as monomeric beta-sheet structures, *Curr. Op. Struct. Biol.* **9** (1999), 487–493.

[28] O. Livnah, E.A. Stura, D.L. Johnson, S.A. Middleton, L.S. Mulcahy, N.C. Wrighton, W.J. Dower, L.K. Jolliffe and I.A. Wilson, Functional mimicry of a protein hormone by a peptide agonist: the EPO receptor complex at 2.8 Å, *Science* **273** (1996), 464–471.
[29] H.B. Lowman, Y.M. Chen, N.J. Skelton, D.L. Mortensen, E.E. Tomlinson, M.D. Sadick, I.C.A. Robinson and R.G. Clark, Molecular mimetics of insulin-like growth factor 1 (IGF-1) for inhibiting IGF-1:IGF-binding protein interactions, *Biochemistry* **37** (1998), 8870–8878.
[30] C. Mattos, G.A. Petsko and M. Karplus, Analysis of two-residue turns in proteins, *J. Mol. Biol.* **238** (1994), 733–747.
[31] A.J. Maynard, G.J. Sharman and M.S. Searle, Origin of β-hairpin stability in solution: structural and thermodynamic analysis of the folding of a model peptide supports hydrophobic stabilization in water, *J. Am. Chem. Soc.* **120** (1998), 1996–2007.
[32] P. Milburn, Y. Konishi, Y. Meinwald and H. Scheraga, Chain reversals in model peptides: Studies of cystine-containing peptides. 1. Conformational free energies of cyclization of hexapeptides of sequence Ac-Cys-X-Pro-Gly-Y-NHMe, *J. Am. Chem. Soc.* **109** (1987), 4486–4496.
[33] P. Milburn, Y. Meinwald, S. Takahashi, T. Ooi and H. Scheraga, Chain reversal in model peptides: studies of cystine-containing cyclic peptides, *Int. J. Peptide Protein Res.* **31** (1988), 311–321.
[34] D.L. Minor and P.S. Kim, Context is a major determinant of β-sheet propensity, *Nature* **371** (1994), 264–267.
[35] D.L. Minor and P.S. Kim, Measurement of the β-sheet-forming propensities of the amino acids, *Nature* **367** (1994), 660–663.
[36] V. Munoz, P.A. Thompson, J. Hofrichter and W.A. Eaton, Folding dynamics and mechanism of beta-hairpin formation, *Nature* **390** (1997), 196–199.
[37] G.R. Nakamura, M.A. Starovasnik, M.E. Reynolds and H.B. Lowman, A novel family of β-hairpin peptides that inhibit IgE activity by binding to the high-affinity IgE receptor, *Biochemistry* **40** (2001), 9828–9835.
[38] K.T. O'Neil and W.F. DeGrado, A thermodynamic scale for the helix-forming tendencies of the commonly occurring amino acids, *Science* **250** (1990), 646–651.
[39] M. Ramírez-Alvarado, F.J. Blanco and L. Serrano, De novo design and structural analysis of a model β-hairpin peptide system, *Nature Struct. Biol.* **3** (1996), 604–611.
[40] J.S. Richardson and D.C. Richardson, Natural beta-sheet proteins use negative design to avoid edge-to-edge aggregation, *Proc. Natl. Acad. Sci. USA* **99** (2002), 2754–2759.
[41] S.J. Russell, T. Blandl, N.J. Skelton and A. Cochran, Stability of cyclic β-hairpins: asymmetric contributions from side chains of a hydrogen-bonded cross-strand resdidue pair, in press.
[42] S.J. Russell and A.G. Cochran, Designing stable β-hairpins: energetic contributions from cross-strand residues, *J. Am. Chem. Soc.* **122** (2000), 12 600–12 601.
[43] C.M. Santiveri, M. Rico and M.A. Jimenez, $^{13}C\alpha$ and $^{13}C\beta$ chemical shifts as a tool to delineate beta-hairpin structures in peptides, *J. Biomolec. NMR.* **19** (2001), 331–345.
[44] M.S. Searle, Peptide models of protein β-sheets: design, folding and insights into stabilizing weak interactions, *J. Chem. Soc., Perkin Trans.* **2** (2001), 1011–1020.
[45] B.L. Sibanda, T.L. Blundell and J.M. Thornton, Conformation of β-hairpins in protein structures. A systematic classification with applications to modelling by homology, electron density fitting and protein engineering, *J. Mol. Biol.* **206** (1989), 759–777.
[46] S.S. Sidhu, H.B. Lowman, B.C. Cunningham and J.A. Wells, Phage display for selection of novel binding peptides, *Methods Enzymol.* **328** (2000), 333–363.
[47] V. Sieber and G.R. Moe, Interactions contributing to the formation of a β-hairpin-like structure in a small peptide, *Biochemistry* **35** (1996), 181–188.
[48] N.J. Skelton, Y.M. Chen, N. Dubree, C. Quan, D.Y. Jackson, A.G. Cochran, K. Zobel, K. Deshayes, M. Baca, M.T. Pisabarro and H.B. Lowman, Structure-function analysis of a phage-derived peptide that binds to IGFBP-1, *Biochemistry* **40** (2001), 8487–8498.
[49] N.J. Skelton, K.C. Garcia, D.V. Goeddel, C. Quan and J.P. Burnier, Determination of the solution structure of guanylin, *Biochemistry* **33** (1994), 13 581–13 592.
[50] N.J. Skelton, S. Russell, F. de Sauvage and A.G. Cochran, Amino acid determinants of beta-hairpin conformation in erythropoeitin receptor agonist peptides derived from a phage display library, *J. Mol. Biol.* **316** (2002), 1111–1125.
[51] C.K. Smith, J.M. Withka and L. Regan, A thermodynamic scale for the β-sheet forming tendencies of the amino acids, *Biochemistry* **33** (1994), 5510–5517.
[52] S. Spera and A. Bax, Empirical correlation between protein backbone conformation and $C\alpha$ and $C\beta^{13}C$ nuclear magnetic resonance chemical shifts, *J. Am. Chem. Soc.* **113** (1991), 5490–5492.
[53] N. Srinivasan, R. Sowdhamini, C. Ramakrishnan and P. Balaram, Conformations of disulfide bidges in proteins, *Int. J. Peptide Protein Res.* **36** (1990), 147–155.
[54] F.A. Syud, H.E. Stanger and S.H. Gellman, Interstrand side chain-side chain interactions in a designed β-hairpin: significance of both lateral and diagonal pairings, *J. Am. Chem. Soc.* **123** (2001), 8667–8677.

[55] C. Vita, E. Drakopoulou, J. Vizzavona, S. Rochette, L. Martin, A. Menez, C. Roumestand, Y.S. Yang, L. Ylisastigui, A. Benjouad and J.C. Gluckman, Rational engineering of a miniprotein that reproduces the core of the CD4 site interacting with HIV-1 envelope glycoprotein, *Proc. Natl. Acad. Sci. USA* **96** (1999), 13 091–13 096.
[56] L. Wang, T. O'Connell, A. Tropsha and J. Hermans, Molecular simulations of beta-sheet twisting, *J. Mol. Biol.* **262** (1996), 283–293.
[57] S.J. Weiner, P.A. Kollman, D.A. Case, U.C. Singh, C. Ghio, G. Alagona, J.S. Profeta and P. Weiner, A new force field for molecular mechanical simulation of nucleic acids and proteins, *J. Am. Chem. Soc.* **106** (1984), 765–784.
[58] S.J. Weiner, P.A. Kollman, D.T. Nguyen and D.A. Case, An all-atom force field for simulations of proteins and nucleic acids, *J. Comput. Chem.* **7** (1986), 230–252.
[59] C.M. Wilmot and J.M. Thornton, Analysis and prediction of the different types of β-turns in proteins, *J. Mol. Biol.* **203** (1988), 221–232.
[60] M.A. Wouters and P.M.G. Curmi, An analysis of side chain interactions and pair correlations within antiparallel β-sheets: the differences between backbone hydrogen-bonded and non-hydrogen-bonded residue pairs, *Proteins* **22** (1995), 119–131.
[61] K. Wüthrich, *NMR of Proteins and Nucleic Acids*, Wiley, New York, 1986.
[62] X. Xu and D.A. Case, Automated prediction of ^{15}N, ^{13}Cα, ^{13}Cβ and ^{13}C$'$ chemical shifts in proteins using a density functional database, *J. Biomolec. NMR* **21** (2002), 321–333.
[63] A.S. Yang and B. Honig, Free energy determinants of secondary structure formation: II. Antiparallel beta-sheets, *J. Mol. Biol.* **252** (1995), 366–376.